

Lyapunov instability of pendulums, chains, and strings

129

William G. Hoover and Carol G. Hoover

Department of Physics, Keio University, Yokohama 223, Japan

Harald A. Posch

Institute for Experimental Physics, University of Vienna, Vienna A-1090, Austria

(Received 2 November 1989)

We investigate both dynamic and time-averaged chaos in a series of problems ranging from a simple pendulum to many-body chains and strings of particles in a gravitational field. Chain and spring systems typically display time-averaged Lyapunov spectra resembling those of one- and two-dimensional statistical-mechanical systems, but with details depending strongly on the nature of the links and the choice of canonical coordinates.

I. INTRODUCTION

The chaotic phase-space mixing caused by Lyapunov instability is the key to understanding thermodynamic irreversibility in mechanical systems.¹ The "static," meaning time-averaged, spectrum of Lyapunov exponents $\{\lambda\}$ describes and defines the chaotic phase-space evolution of exponentially unstable dynamical systems, as follows: the largest exponent λ_1 describes the time-averaged rate at which nearby phase-space trajectories separate; adding on further exponents $\lambda_2, \lambda_3, \lambda_4, \dots$ gives sums describing the expansion or contraction rates of corresponding two-, three-, four-, . . . dimensional phase-space objects. Thus the individual exponents, ordered from largest to smallest $\lambda_1 > \lambda_2 > \lambda_3 > \dots$, represent the static time-averaged values of dynamic local orthogonal deformation rates in the neighborhood of a phase-space trajectory. The dynamic deformation is most naturally followed and described in a comoving, and corotating, coordinate system centered on such a trajectory. Several numerical methods for generating and averaging the dynamic values in order to obtain the static exponents have been developed and applied.²⁻⁶

Static Lyapunov spectra have recently been obtained for a variety of equilibrium and nonequilibrium systems of interest in statistical mechanics. Fluids and solids in one, two, and three space dimensions have been investigated.⁷⁻⁹ The time-averaged results found so far have few distinctive features. The qualitative shapes of the spectra can be roughly described by power laws reminiscent of Debye's crystal-frequency distributions and varying with system dimensionality, thermodynamic phase, and boundary conditions, including temperature, but failing to show any of the rich diversity characterizing solid-state frequency spectra.

Because these static time-averaged properties reveal little of the complex details which distinguish one dynamical system from another, it seemed to us worthwhile to examine the dynamically varying local structure of the Lyapunov spectra. Our previous investigation¹⁰ of time dependence treated the classic Lorenz model,¹¹ which in-

troduced chaos to a wide audience a generation ago. Here we extend our time-dependent studies to a class of systems bridging the gap between mechanics and many-body statistical mechanics: pendulums, chains, and strings. These models are well suited to analysis.

In the following sections we analyze the dynamic phase-space structure associated with Lyapunov-unstable pendulum systems. Our calculations establish that this structure varies from one canonical coordinate system to another and typically exhibits an interesting time-symmetry property closely related to Liouville's theorem. In Sec. II we describe the calculations establishing these results. Section III is a summary and a record of our conclusions.

II. MANY-BODY SIMULATIONS AND RESULTS

One might suspect that an isolated single-pendulum system would have no interesting dynamical properties. If the pendulum is rigid, this is true. An isolated *rigid* single pendulum is an integrable system, with a periodic one-dimensional orbit making up its one-dimensional constant-energy phase-space trajectory. But the problem becomes interesting as soon as another degree of freedom is added. Adding one more degree of freedom expands the accessible constant-energy phase-space region to three dimensions and makes chaotic motion at least possible. The additional degree of freedom can come from relaxing the rigidity constraint, from adding another mass, from making the pendulum spherical and adding a constraint, or from external driving. Any of these four sources can lead to chaos. Making the pendulum linkage flexible rather than rigid is the simplest.

We find that the motion of a single flexible pendulum can be chaotic, for some energies. Consider the simplest possible example: a single Hooke's-law pendulum, with a spring energy ϕ given by

$$\phi = (\kappa/2)(r-1)^2,$$

with the force constant $\kappa=4$, and with initial conditions providing just enough energy to reach the unstable verti-

cal configuration with zero stored spring energy ϕ and spring length equal to the rest length l .

We applied Benettin's method to this chaotic flexible-pendulum problem so as to determine all four time-averaged Lyapunov exponents and to characterize as well their dynamic probability densities. The calculation proceeds by following the motion of four orthonormal basis vectors in the phase space $\{\delta_1, \delta_2, \delta_3, \delta_4\}$ and measuring their tendency to grow or shrink, as is described in Refs. 2-4. These comoving local rates of growth, when time-averaged, give the static Lyapunov spectrum. The result of this numerical calculation establishes that the time-averaged Lyapunov spectrum is

$$\{\lambda\} = (0.128, 0.000, -0.000, -0.128),$$

with statistical uncertainties in the four exponents of ± 0.002 . We checked these results by carrying out parallel calculations in Cartesian and polar coordinates. Independent calculations were carried out at Keio University and at the University of Vienna.

Consider next the dynamical Lyapunov spectrum for this same system. For this simple flexible-pendulum case probability *densities*, obtained by binning the time-varying instantaneous values of the Lyapunov growth and decay rates, are shown in Fig. 1. In view of the symmetry of these densities, with $P(\lambda_1) = P(-\lambda_4)$ and $P(\lambda_2) = P(-\lambda_3)$, only those for λ_1 and λ_2 are shown in Fig. 1. Note that the dynamic exponent densities depend upon the choice of coordinates. Results for both Cartesian and polar coordinates are shown in the figure. Throughout this paper we use the same notation λ for both the time-varying growth rates and the correspond-

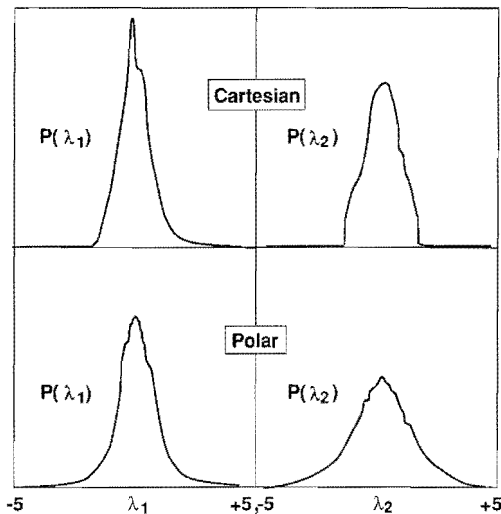


FIG. 1. Probability densities for the instantaneous Lyapunov exponents (dynamic exponential expansion rates) found for the chaotic flexible single pendulum with the force constant κ set equal to 4 and just sufficient energy to reach the fully extended vertical configuration. Only $P(\lambda_1) = P(-\lambda_4)$ and $P(\lambda_2) = P(-\lambda_3)$ are shown, at the left and right, respectively, because the symmetry of the distributions applies to the instantaneous values just as well as to the time-averaged values shown here. Results are shown for both Cartesian (top) and polar (bottom) representations of the system.

ing time averages, trusting that the distinction between the two is clear by context. The widths of the dynamic distributions are up to ten times the static (time-averaged) value of the largest Lyapunov exponent λ_1 . The rms fluctuations about the mean values given above are $\langle \lambda_1 \rangle_{\text{rms}} = \langle \lambda_4 \rangle_{\text{rms}} = 0.71$ and $\langle \lambda_2 \rangle_{\text{rms}} = \langle \lambda_3 \rangle_{\text{rms}} = 0.75$ for Cartesian coordinates and $\langle \lambda_1 \rangle_{\text{rms}} = \langle \lambda_4 \rangle_{\text{rms}} = 0.96$ and $\langle \lambda_2 \rangle_{\text{rms}} = \langle \lambda_3 \rangle_{\text{rms}} = 1.26$ for polar coordinates.

It is remarkable that the dynamic fluctuations depend strongly upon the coordinate system chosen for the calculation while the static mean values cannot.²⁻⁶ Fundamentally, this striking feature of our results reflects the time-varying direction of separation of two nearby trajectories. For two definite trajectories the direction continually fluctuates, reflecting the changing sensitivity of the trajectories' separation to the various canonical coordinates and momenta. On the other hand, for times long enough to determine the static values, the logarithmic time-averaged growth rates have roughly equal (because of the logarithm) projections on all the phase-space axes. In the longtime limit the rates are independent of the choice of coordinates but the fluctuations are not.

The symmetry implicit in the two time-averaged densities shown in Fig. 1, with $P(\lambda_1) = P(-\lambda_4)$ and $P(\lambda_2) = P(-\lambda_3)$, is real, and follows from Liouville's theorem. It develops dynamically in an interesting way. After an initial asymmetric transient, which depends on the initial choices of the δ vectors and typically lasts a few thousand time steps, the four orthonormal four-dimensional δ vectors converge to a stable arrangement in which pairs of instantaneous Lyapunov exponents, not just their time averages, have identical absolute values, with $|\lambda_1| = |\lambda_4|$ and $|\lambda_2| = |\lambda_3|$. This feature occurs here with either coordinate system, and generally, for many-body as well as few-body systems. We believe that the time required for this property corresponds roughly to the time required for finite-precision integration to lose memory of the initial conditions. The time required for this memory loss greatly exceeds the oscillation time and the Lyapunov time; both these times are of order 10, which is 1000 typical time steps.

Even a single flexible pendulum has interesting chaotic properties, illustrating the dependence of dynamic Lyapunov exponents, but not their static averages, on coordinate system, and exhibiting as well this nice dynamic symmetry property.

When we described the dependence of fluctuations on the coordinate choice to a colleague, he asserted that "Cartesian coordinates are the natural choice." But even the Cartesian situation is not simple. Consider, for instance, a more general Hamiltonian for the flexible Hookean pendulum, including a scale factor s , so that new canonical Cartesian coordinates $Q = qs$ and momenta $P = p/s$ can be defined without changing either the value of the Hamiltonian or the underlying dynamics,

$$H(s) = (Ps)^2/2 + (\kappa/2)[(R/s) - 1]^2 + (Y/s).$$

A numerical investigation, for the same energy and trajectory described above and illustrated in Fig. 1, reveals that the fluctuations in the Lyapunov spectrum increase

away from the value of s (roughly $s=2$) at which they are minimized while the mean values of the exponents are unchanged. This simple example suggests that if there is a “natural choice” of coordinates, it is that Cartesian frame which minimizes the fluctuations. Likewise, simply switching from the cgs to the mks system of units for length and momentum modifies the direction, and hence the fluctuations, for the dynamic Lyapunov-exponent vectors.

The sensitivity to coordinate system can be analyzed analytically for the one-dimensional harmonic oscillator, an integrable system for which both the time-averaged Lyapunov exponents vanish. For the oscillator Hamiltonian with scale parameter s ,

$$H(s) = [(Ps)^2 + (Q/s)^2]/2,$$

diligent application of the analytic Lagrange-multiplier methods developed in Refs. 3 and 4 leads to the simple result

$$\langle \lambda^2 \rangle = (s^{+1} - s^{-1})^2 / 2.$$

Thus unless s is chosen equal to the “natural” value 1 for which P^2 and Q^2 have equal time averages, even the Cartesian-frame harmonic-oscillator Lyapunov exponents have frame-dependent nonzero fluctuations.

The alternative to introducing chaos with a flexible pendulum link is to add more degrees of freedom, keeping the links rigid, either by adding links, by increasing the number of spatial dimensions, or by driving the pendulum with an external force. The topology of chaos in the rigid double pendulum has already been nicely characterized,¹² the three-dimensional spherical pendulum, with an additional constraint, has been studied both experimentally and computationally,¹³ and the dynamics of a driven pendulum is by now well known.¹⁴ An idealized double pendulum is shown in Fig. 2, where we arbitrarily choose the two lengths equal to unity. In our classroom-demonstrator version the lower pendulum was made slightly shorter than the upper pendulum (which is shaped like an inverted U) in order to make all pairs of the angles α and β , shown in the figure, accessible. With rigid links between the masses the two degrees of freedom

can be chosen in many ways. The two simplest choices are illustrated in the figure.

The textbook coordinate system used by Landau and Lifshitz¹⁵ is reproduced in Fig. 2(a). This choice is the one most easily generalized to the many-pendulum case. For convenience, and to avoid the clutter of extraneous symbols, we simply state here that the masses m_1 and m_2 , lengths l_1 and l_2 , and gravitational field strength g are all chosen equal to unity. The more general case is a simple extension of the prototypical cases studied here. Thus the double-pendulum Lagrangian becomes

$$L_B = 2 \cos \alpha + \cos(\alpha + \beta) + \left[\frac{d\alpha}{dt} \right]^2 + \frac{1}{2} \left[\frac{d\alpha}{dt} + \frac{d\beta}{dt} \right]^2 + \frac{d\alpha}{dt} \left[\frac{d\alpha}{dt} + \frac{d\beta}{dt} \right] \cos(\beta).$$

Richter and Scholz¹² used the alternative coordinate system shown in Fig. 1(b), with the Lagrangian

$$L_B = 2 \cos \alpha + \cos(\alpha + \beta) + \left[\frac{d\alpha}{dt} \right]^2 + \frac{1}{2} \left[\frac{d\alpha}{dt} + \frac{d\beta}{dt} \right]^2 + \frac{d\alpha}{dt} \frac{d\alpha}{dt} + \frac{d\beta}{dt} \cos(\beta).$$

The two choices just given, plus ordinary polar coordinates, were helpful in providing equivalent numerical checks for our exploratory calculations of the time-averaged Lyapunov spectra.

More complex double-pendulum systems result if the rigid constraints just discussed are replaced by Hooke's-law springs. As has been emphasized repeatedly,¹⁶ the phase-space probability density for such a system differs from the constrained probability density even in the limit that the springs are infinitely stiff. The short-time dynamics as well as the static and dynamic values of the Lyapunov exponents are also qualitatively different. Using Hookean springs rather than constraints, the four-dimensional phase space becomes eight dimensional and a typical chaotic trajectory has three exponents with positive time-averaged values, three with negative values and two with zero.

Over a wide range of energy (relative to the accessible gravitational energy) the rigid double-pendulum motion is now known to be chaotic.¹² Just as in the Hooke's-law case mentioned above, the rigid-pendulum spectrum also becomes instantaneously symmetric after a transient period of a few thousand time steps. In the four-dimensional phase space an infinitesimal comoving and corotating hypersphere distorts into a hyperellipsoid with one diverging axis [with time average varying as $\exp(\lambda_1 t) \equiv \exp(\lambda t)$], two neutral axes, varying as $\exp(\lambda_2 t) = \exp(\lambda_3 t) \equiv 1$, and one converging axis [varying as $\exp(\lambda_4 t) \equiv \exp(-\lambda t)$]. It is true that the dynamics could be followed in a three-dimensional projection of phase space, by taking energy conservation into account, but in the projected space Liouville's theorem is no longer satisfied instantaneously so that the analysis required to compute the Lyapunov exponents becomes more complicated.

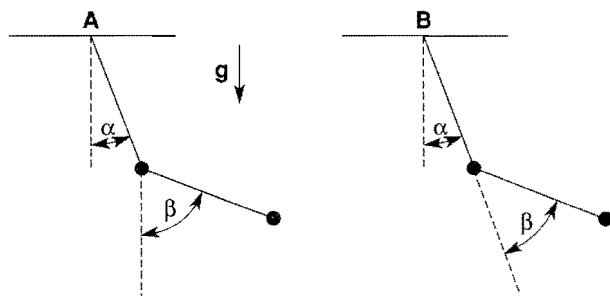


FIG. 2. Alternative generalized-coordinate systems used in describing the double-pendulum system with the Lagrangians L_A and L_B defined in the text. Exploratory calculations were carried out in both these frames, as well as with standard polar coordinates, in order to eliminate programming errors.

The mathematics of the many-body problem can be simplified, and the need for solving a large system of linear equations can be entirely avoided, by adopting Hooke's-law springs to link the masses rather than applying rigid Lagrangian constraints. The two simplest types of such spring systems link together similar masses $m_1 = m_2 = \dots = m_n = m$, or, alternatively, very light masses $m_1 = m_2 = \dots = m_{n-1} = m$, which support a heavier mass $M \gg m$. In the first case, which corresponds to a heavy chain in a gravitational field, the time average of the vertical component of tension in the chain increases linearly with the mass supported so that the vertical load on the uppermost springs averages N times that supported by the bottom spring. The second case, which corresponds to a massless string supporting a heavy weight, can be modeled by allowing only the last of the n masses to interact with the gravitational field. In this way the average vertical load on each spring is the same.

Again, for convenience and simplicity, in what follows we set the masses, rest lengths of the springs, and the strength of the gravitational field all equal to unity. Just as before, the stiff springs obey Hooke's law

$$\phi = (\kappa/2)(r-1)^2.$$

The natural spring frequency varies as the square root of the force constant κ . We were able to treat κ values as high as 10 000 000 by reducing the fourth-order Runge-Kutta timestep from 0.01 to 0.0001. With that method none of the problems described here presented numerical difficulties in conserving the energy or in satisfying the constraints.

In Fig. 3 we display dynamic double-pendulum probability-density histograms for two Hookean-spring cases $\kappa=4$ and 64. The mean values over these histograms, indicated in the figure, correspond to the time-averaged Lyapunov exponents. Again the instantaneous spectra become exactly symmetric, after a short time, so that we show only the distribution for the four largest exponents. Notice particularly that the fluctuations about

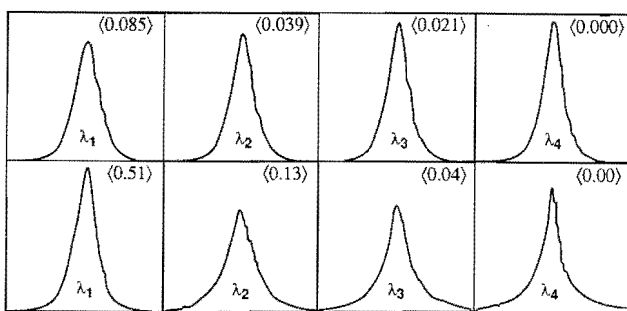


FIG. 3. Cartesian-coordinate probability densities for the flexible double-pendulum instantaneous Lyapunov exponents (dynamic exponential expansion rates) $\lambda_1, \dots, \lambda_4$ (left to right) with Hooke's-law spring constants κ equal to 4 (top) and 64 (bottom). The distributions for the remaining exponents $\lambda_5, \dots, \lambda_8$ are mirror images of those shown in the figure. The abscissa values vary from -5 to $+5$ for $\kappa=4$ and from -25 to $+25$ for $\kappa=64$.

the mean are about five times larger for the larger force constant κ . This shows that the vibrational motion of the springs themselves, with a frequency of order $(\kappa/m)^{1/2}$, mixes with the slower Lyapunov instability frequency. Because the high-frequency fluctuations are relatively regular, accurate values for the means, the static Lyapunov spectrum, can still be obtained.

The fluctuations in the instantaneous dynamical values of the rigid-pendulum Lyapunov exponents are relatively smaller than their flexible-pendulum counterparts. Consider again the rigid lecture-demonstration double pendulum, initially motionless and stretched out horizontally. In this case the time-averaged static Lyapunov exponents have magnitudes 0.30, 0.00, 0.00, and -0.30 (again with units such that lengths, masses, and gravitational fields are all set equal to unity). The dynamic root-mean-squared fluctuations about these static mean values are 0.84 for λ_1 and λ_4 , and 0.79 for λ_2 and λ_3 , using the Landau-Lifshitz coordinate system.

Because the mathematics is simpler, we confined our many-mass simulations to flexible pendulums. We investigated a series of strings with 2, 4, 8, and 16 masses, all interacting with nearest-neighbor force constants $\kappa=4$ or 64, and with only the last of the masses interacting with a gravitational field, of unit strength. We found the time-averaged spectra listed in Table I and plotted in such a way as to emphasize the rapid convergence toward the static spectrum for a continuous string, in Fig. 4. The static distributions show again that the fluctuating growth rates include mixing from the harmonic degrees of freedom in the springs, with the high-frequency-spring fluctuations nearly an order of magnitude higher than the low-frequency ones.

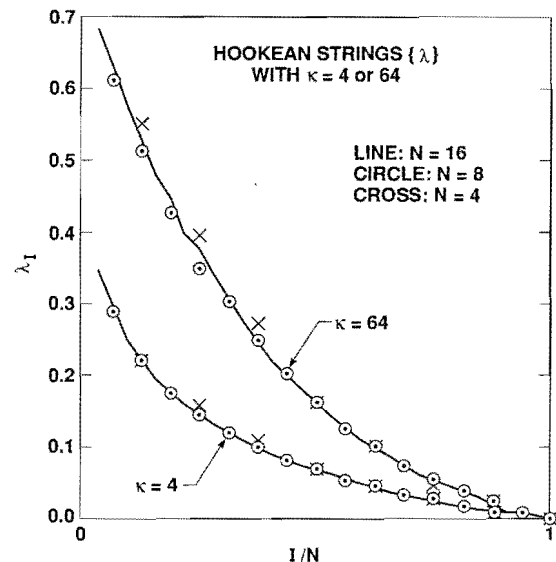


FIG. 4. Distribution of Lyapunov exponents for strings with $N=2, 4, 8$, and 16 masses using Cartesian coordinates. The initial configuration is motionless and horizontal. Only the last mass in the chain interacts with the gravitational field. The N largest values of the Lyapunov exponents $\{\lambda_j\} = \lambda_1 > \lambda_2 > \lambda_3 > \dots > \lambda_N$ are plotted as a function of the dimensionless ratio $1/N$; thus the abscissa values vary from $1/N$ to 1.

TABLE I. Lyapunov spectra ($2N$ of the $4N$ exponents) for strings of N units masses connected by Hookean springs with force constants all equal to $\kappa=4$ or 64. Only the last mass interacts with a vertical gravitational field and the initial condition was fully extended and horizontal. The mean-squared values were calculated using Cartesian coordinates. The time averages are for the last 400 000 timesteps of 600 000 step runs with a fourth-order Runge-Kutta $dt=0.005$. The uncertainties in the exponents do not exceed ± 0.01 .

		Exponents							
		$\kappa=4$							
$\{\lambda\}_2$	0.08	0.04	0.02	0.00					
$\{\lambda^2\}_2$	1.10	0.75	0.80	0.80					
$\{\lambda\}_4$	0.23	0.16	0.11	0.07	0.05	0.03	0.01	0.00	
$\{\lambda^2\}_4$	0.68	0.63	0.59	0.64	0.69	0.64	0.65	0.73	
$\{\lambda\}_8$	0.29	0.21	0.16	0.15	0.12	0.10	0.08	0.07	
	0.05	0.05	0.03	0.03	0.02	0.01	0.00	0.00	
$\{\lambda^2\}_8$	0.56	0.39	0.35	0.32	0.33	0.35	0.34	0.40	
	0.37	0.40	0.39	0.42	0.40	0.43	0.47	0.49	
$\{\lambda\}_{16}$	0.35	0.29	0.25	0.22	0.19	0.18	0.16	0.14	
	0.13	0.12	0.11	0.10	0.09	0.08	0.08	0.07	
	0.06	0.05	0.05	0.04	0.04	0.04	0.03	0.03	
	0.02	0.02	0.01	0.01	0.01	0.00	0.00	0.00	
$\{\lambda^2\}_{16}$	0.60	0.41	0.34	0.26	0.24	0.22	0.23	0.22	
	0.21	0.20	0.20	0.20	0.21	0.21	0.21	0.22	
	0.23	0.24	0.24	0.26	0.25	0.22	0.24	0.25	
	0.26	0.27	0.25	0.23	0.28	0.22	0.26	0.20	
		$\kappa=64$							
$\{\lambda\}_2$	0.51	0.13	0.05	0.00					
$\{\lambda^2\}_2$	21	58	88	180					
$\{\lambda\}_4$	0.55	0.40	0.27	0.16	0.10	0.05	0.03	0.00	
$\{\lambda^2\}_4$	13	19	28	43	64	90	92	144	
$\{\lambda\}_8$	0.62	0.51	0.43	0.35	0.30	0.25	0.20	0.16	
	0.13	0.09	0.07	0.05	0.04	0.03	0.01	0.00	
$\{\lambda^2\}_8$	8	8	10	11	13	16	19	24	
	31	37	45	52	61	63	83	92	
$\{\lambda\}_{16}$	0.69	0.63	0.58	0.53	0.48	0.45	0.40	0.38	
	0.34	0.30	0.28	0.25	0.22	0.20	0.18	0.16	
	0.14	0.12	0.11	0.10	0.09	0.08	0.06	0.06	
	0.05	0.04	0.03	0.02	0.02	0.01	0.00	0.00	
$\{\lambda^2\}_{16}$	5	5	5	5	5	6	6	6	
	7	8	8	9	10	11	12	13	
	16	16	18	21	22	24	28	30	
	32	38	38	39	43	42	50	49	

III. CONCLUSIONS

Distributions of dynamic Lyapunov spectra of the type simulated here should prove helpful in distinguishing among classes of dynamical systems and in identifying the particular coordinate systems best suited to their study. In an oversimplified and unrealistic view of phase-space dynamics, dynamic Lyapunov exponents would be constants of the motion, equal to the static values. In reality the dynamic contributions to the static exponents vary, but are at least reproducible smoothly varying point functions in phase space, depending on the recent past history of the trajectory. But the numerical values of these dynamic point functions, as well as the orientations of the corresponding Lyapunov δ vectors, depend on the chosen phase space. Simple examples, such as the single chaotic flexible pendulum and the in-

tegrable one-dimensional oscillator, show that the coordinate system used to describe these point functions affects their fluctuation over a long orbit. This means that the local time-varying contributions to the Lyapunov exponents do not provide an unambiguous chaos mechanism or a means of locating bifurcation sites in phase space. Such appealing ideas can at best be approximations.

Here we also find a wide dynamic variation of the exponent contributions with time which depends on the strength of the underlying harmonic vibrational frequencies. The coordinate-independent time-averaged spectra found here resemble those already known from one- and two-dimensional many-body studies. To a very rough approximation they are power laws, but the deviations are significant.

Our calculations of instantaneous Lyapunov spectra il-

lustrated another interesting general property in all of the coordinate systems we investigated. It is generally the case that, after a transient period of several "Lyapunov times"—that is, several times $1/\lambda_1$ —the initial choice of δ vectors becomes irrelevant and the instantaneous spectrum of dynamic exponents (expansion rates) becomes symmetric. This is an equilibrium constant-energy property and is a recognized consequence of the general time symmetry which underlies Liouville's theorem. The corresponding symmetry is nevertheless dynamically unstable and hence necessarily absent in systems exhibiting dissipation (*even when the equations of motion are time reversible*), for which the time-averaged summed values of the negative Lyapunov exponents always exceed those of the averaged summed positive exponents in absolute value. See, for instance, Ref. 10.

The probability densities of the instantaneous expansion rates, the "dynamic Lyapunov exponents" appear to us to contain more information, in a readily computable form, than does the currently popular multifractal representation. But because the dynamic exponent densities depend upon coordinate system, their use requires judgment in selecting the "most natural" frame.

The systems studied here are useful in introducing chaos in that both the single and double pendulums are well suited to classroom demonstration. Our results show that even a single pendulum, when constrained by a spring, can exhibit widespread chaotic behavior if the spring is not too stiff.

ACKNOWLEDGMENTS

We thank Professor Boku, Professor Kawai, and Professor Nosé for support and for help with the computer facilities at Keio University and at the University of Tokyo. Our calculations at Vienna were carried out within the framework of the IBM European Supercomputing Initiative at the University of Vienna Computer Center. We are grateful for this support. Conversations with Professor Nosé were most helpful. A part of this work was performed under the auspices and with the support of the Department of Energy and the Lawrence Livermore National Laboratory, under Contract No. W-7405-Eng-48. Our work in Japan was financed by a grant from the Japan Society for the Promotion of Science.

¹B. L. Holian, W. G. Hoover, and H. A. Posch, *Phys. Rev. Lett.* **59**, 10 (1987).

²G. Benettin, L. Galgani, and J.-M. Strelcyn, *Phys. Rev. A* **14**, 2338 (1976); G. Benettin, L. Galgani, A. Giorgilli, and J.-M. Strelcyn, *Meccanica* **15**, 9 (1980).

³W. G. Hoover and H. A. Posch, *Phys. Lett. A* **113**, 82 (1985).

⁴W. G. Hoover and H. A. Posch, *Phys. Lett. A* **123**, 227 (1987).

⁵A. Wolf, J. B. Swift, H. L. Swinney, and J. A. Vastano, *Physica D* **16**, 285 (1985).

⁶J.-P. Eckmann and D. Ruelle, *Rev. Mod. Phys.* **57**, 617 (1985).

⁷R. Livi, M. Pettini, S. Ruffo, and A. Vulpiani, *J. Stat. Phys.* **48**, 539 (1987).

⁸W. G. Hoover and H. A. Posch, *J. Chem. Phys.* **87**, 6665 (1987).

⁹H. A. Posch and W. G. Hoover, *Phys. Rev. A* **38**, 473 (1988).

¹⁰W. G. Hoover, C. G. Tull, and H. A. Posch, *Phys. Lett. A* **131**, 211 (1988).

¹¹E. N. Lorenz, *J. Atmos. Sci.* **20**, 130 (1963).

¹²P. H. Richter and H. J. Scholz, in *Stochastic Phenomena and Chaotic Behavior in Complex Systems*, edited by P. Schuster (Springer-Verlag, Berlin, 1984).

¹³R. D. Peters, *Phys. Rev. A* **38**, 5352 (1988).

¹⁴H. G. Schuster, *Deterministic Chaos, An Introduction*, 2nd revised ed. (VCH Verlagsgesellschaft, Weinheim, 1988).

¹⁵L. D. Landau and E. M. Lifshitz, *Mechanics* (Pergamon, Oxford, 1960).

¹⁶N. G. van Kampen and J. J. Lodder, *Am. J. Phys.* **52**, 419 (1984).